

RESEARCH ARTICLE | JANUARY 14 2008

***In situ* H₂S passivation of In_{0.53} Ga_{0.47} As / In P metal-oxide-semiconductor capacitors with atomic-layer deposited Hf O₂ gate dielectric** ✓

E. O'Connor; R. D. Long; K. Cherkaoui; K. K. Thomas; F. Chalvet; I. M. Povey; M. E. Pemble; P. K. Hurley; B. Brennan; G. Hughes; S. B. Newcomb



Appl. Phys. Lett. 92, 022902 (2008)

<https://doi.org/10.1063/1.2829586>



Articles You May Be Interested In

Comparison of the interfacial and electrical properties of HfAlO films on Ge with S and GeO₂ passivation

Appl. Phys. Lett. (April 2011)

Aluminum oxynitride interfacial passivation layer for high-permittivity gate dielectric stack on gallium arsenide

Appl. Phys. Lett. (November 2006)

Metal gate- Hf O₂ metal-oxide-semiconductor capacitors on n - Ga As substrate with silicon/germanium interfacial passivation layers

Appl. Phys. Lett. (November 2006)

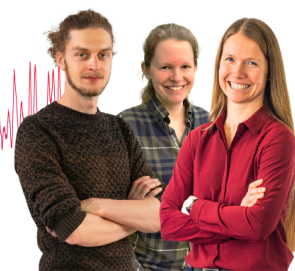
Webinar From Noise to Knowledge

May 13th – Register now



Zurich
Instruments

Universität
Konstanz



***In situ* H₂S passivation of In_{0.53}Ga_{0.47}As/InP metal-oxide-semiconductor capacitors with atomic-layer deposited HfO₂ gate dielectric**

E. O'Connor, R. D. Long, K. Cherkaoui, K. K. Thomas, F. Chalvet, I. M. Povey, M. E. Pemble, and P. K. Hurley^{a)}
Tyndall National Institute, University College Cork, Lee Maltings, Prospect Row, Cork, Ireland

B. Brennan and G. Hughes
School of Physics, Dublin City University, Glasnevin, Dublin 9, Ireland

S. B. Newcomb
Glebe Scientific, Ltd., Newport, County Tipperary, Ireland

(Received 13 July 2007; accepted 7 December 2007; published online 14 January 2008)

We have studied an *in situ* passivation of In_{0.53}Ga_{0.47}As, based on H₂S exposure (50–350 °C) following metal organic vapor phase epitaxy growth, prior to atomic layer deposition of HfO₂ using Hf[N(CH₃)₂]₄ and H₂O precursors. X-ray photoelectron spectroscopy revealed the suppression of As oxide formation in air exposed InGaAs surfaces for all H₂S exposure temperatures. Transmission electron microscopy analysis demonstrates a reduction of the interface oxide between the In_{0.53}Ga_{0.47}As epitaxial layer and the amorphous HfO₂ resulting from the *in situ* H₂S passivation. The capacitance-voltage and current-voltage behavior of Pd/HfO₂/In_{0.53}Ga_{0.47}As/InP structures demonstrates that the electrical characteristics of samples exposed to 50 °C H₂S at the end of the metal-organic vapor-phase epitaxy In_{0.53}Ga_{0.47}As growth are comparable to those obtained using an *ex situ* aqueous (NH₄)₂S passivation. © 2008 American Institute of Physics.
[DOI: 10.1063/1.2829586]

In order to continue complementary metal oxide semiconductor (CMOS) development beyond the 22 nm node, alternative channel materials in combination with high dielectric constant (*k*) gate layers are currently under investigation. One of these approaches is to use high-mobility III-V materials such as InGaAs and GaAs as channel layers.^{1–6} High mobility substrates offer the potential for increased transconductance at reduced voltages, increasing performance at supply voltages ≤1 V. However, a significant factor which has inhibited the use of such materials is the lack of stable, high quality gate insulators on III-V channels. A gate oxide is required with high dielectric constant and sufficiently low density of interface states to avoid Fermi level pinning at the interface with the III-V substrate. As atomic layer deposition (ALD) of high-*k* dielectrics on Si is becoming a reality in manufactured devices, recent research is investigating this approach for use in III-V based devices.^{7,8} A number of groups have also investigated surface passivation of the In_xGa_{1-x}As substrate prior to oxide deposition.^{9–11} *In situ* gaseous passivation is preferable to *ex situ* aqueous techniques which are more likely to introduce contaminants such as C, Na, and heavy metals, as well as increasing InGaAs surface roughness. In addition, both ALD and MOVPE are more attractive techniques than MBE for use in manufacturing technology. In this letter, we evaluate an *in situ* passivation performed at the end of the MOVPE growth of high indium content lattice matched In_{0.53}Ga_{0.47}As grown on InP substrates. The technique is based on the exposure of the In_{0.53}Ga_{0.47}As surface to H₂S at the end of the growth process, prior to gate dielectric formation. The approach is particularly suited to MOVPE III-V growth as H₂S is used as a *n*-type dopant source for InGaAs. The gate oxide employed

in this work is ALD grown HfO₂ using the metal organic precursor Hf[N(CH₃)₂]₄.¹²

In_{0.53}Ga_{0.47}As lattice-matched epitaxial layers of thickness 2 μm and S doped to 4 × 10¹⁷/cm³, were grown in a MOVPE system immediately following growth of a 0.1 μm InP buffer layer (S doped, 2 × 10¹⁸/cm³) on *n*-type InP(100) wafers (S doped, (1–3) × 10¹⁸/cm³). *In situ* passivation of the InGaAs surface was performed in the MOVPE chamber immediately after growth by flowing H₂S over the samples at a flow-rate of 0.1 SCCM (SCCM denotes cubic centimeter per minute at STP), at three different temperatures (50, 200, or 350 °C), for 90 min in a H₂ carrier gas. Subsequently the wafers were moved to an *ex situ* ALD reactor involving ~90 s ambient exposure. HfO₂ layers (~3–~15 nm) were deposited at a temperature of 250 °C by alternating pulses of H₂O and the HfO₂ precursor Hf[N(CH₃)₂]₄, the initial pulse being that of the Hf precursor. MOS structures were completed by vacuum evaporation of ~100 nm of Pd using a deposition rate of 2.5 Å/s, and lift-off, to define capacitors of various areas. No Ohmic back contacts to the InP were formed. *Ex situ* aqueous sulfur (S) passivation was performed in ambient by dipping InGaAs/InP samples in (NH₄)₂S diluted to 20% in de-ionized water at ~60 °C for 20 min. The Pd/HfO₂/In_{0.53}Ga_{0.47}As/InP structures examined in this work experienced no annealing following either dielectric deposition or gate metal formation.

Passivated InGaAs surfaces were studied using x-ray photoelectron spectroscopy (XPS), following ~60 s ambient exposure before loading to the XPS system, to evaluate the effectiveness of the *in situ* passivation approach in suppressing native oxide regrowth. XPS spectra of a sample passivated using *ex situ* aqueous (NH₄)₂S are also included for comparison. Figure 1(a) shows a comparison of the S 2s peak for all samples. XPS does detect S on the InGaAs surface for both the 350 °C *in situ* passivated sample and the *ex*

^{a)}Electronic mail: paul.hurley@tyndall.ie.

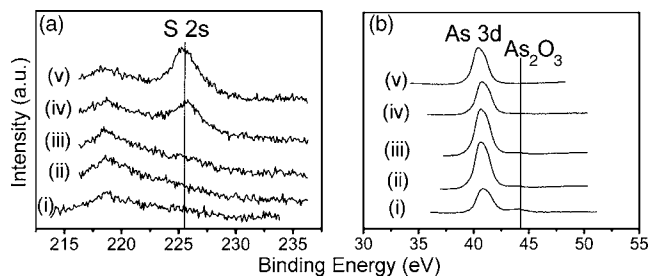


FIG. 1. XPS spectra of (a) the S 2s peak and (b) the As 3d peak for (i) unpassivated InGaAs, (ii) 50 °C, (iii) 200 °C, (iv) 350 °C *in situ* H₂S passivated InGaAs, and (v) *ex situ* aqueous (NH₄)₂S passivated InGaAs.

situ aqueous S passivated sample, but in the case of the 50 and 200 °C *in situ* passivated samples no S is detected on the surface. XPS spectra of the As 3d core level for the unpassivated and passivated samples are shown in Fig. 1(b). This XPS peak is selected to examine the effect of the passivation on suppressing native oxide growth due to the large chemical shift between the As 3d peak and that of the arsenic oxide. In the case of the unpassivated sample, a peak is observed at ~45 eV and assigned to As₂O₃. In the case of all the *in situ* passivated samples this peak is not evident, indicating that this approach is effective in preventing As₂O₃ formation on the InGaAs surface. This is desirable as it has been reported that the unstable As₂O₃ can react to form elemental As which results in Fermi level pinning.^{10,13} The absence of S on the surface of the 50 and 200 °C samples and the fact that As₂O₃ formation was inhibited on both, indicate that S may not be the primary passivating element in this process.

Figure 2(a) compares high frequency capacitance voltage (CV) curves for the unpassivated device and the various *in situ* passivation approaches for a nominal ALD HfO₂ thickness of 9 nm. The minimum capacitance (C_{\min}), at $V_g = -2$ V, is approaching the expected theoretical value of 0.0019 F/m², calculated for these structures assuming inversion at the InGaAs/HfO₂ interface.¹³ The device fabricated on the 50 °C *in situ* passivated surface (50 °C device) displays the highest maximum capacitance in accumulation (C_{\max}) and also exhibits the sharpest transition from depletion to accumulation. The inset of Fig. 2(a) shows the current density-voltage (JV) characteristics for unpassivated and *in situ* passivated MOS structures. All structures exhibit low leakage current density ($<5 \times 10^{-7}$ A/cm² at $V_{fb}+1$ V), demonstrating that these ALD HfO₂ films on InGaAs are highly insulating. It is lowest in the case of the 50 °C device, $\sim 5 \times 10^{-8}$ A/cm² at $V_{fb}+1$ V. Figure 2(b) shows multifrequency CV curves measured over the range of 1 kHz–1 MHz for the 50 °C device. The low frequency CV behavior observed in the 1 kHz curve has been reported previously in narrow bandgap materials.^{14–16} The inset of Fig. 2(b) shows the CV hysteresis curve for the 50 °C device, which has the lowest measured hysteresis, ~380 mV around C_{fb} . These levels of frequency dispersion and hysteresis are to be expected as no postdeposition thermal anneal was performed on these MOS structures.⁹ The fact that the 50 °C passivated device, which XPS showed to have no detectable S signal at the surface, displays the best electrical properties is further evidence that S is not the primary passivating element for the *in situ* process. It is possible to speculate that hydrogen may be passivating the InGaAs surface. One possibility is low temperature dissociative adsorption of H₂S to produce H–S and H species which may bond to As at the

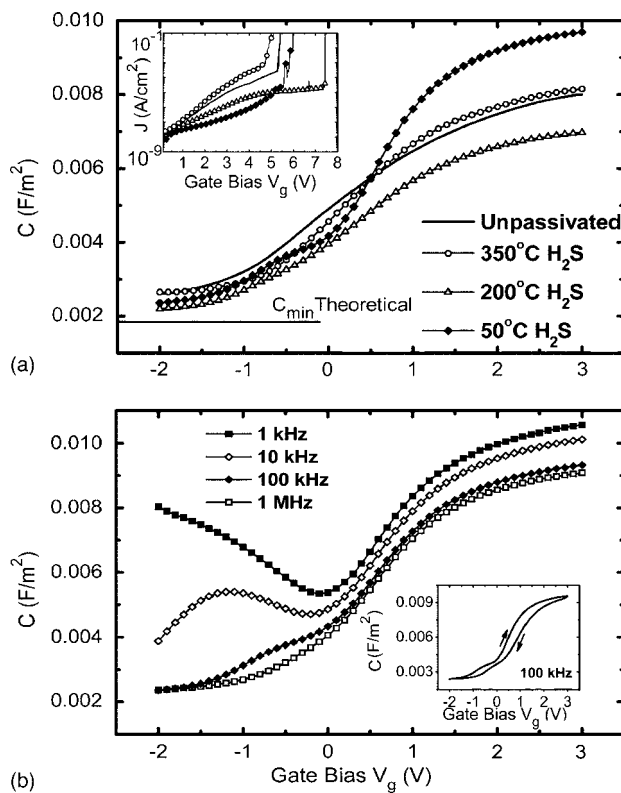


FIG. 2. (a) High frequency (100 kHz) capacitance-voltage characteristics and inset leakage current density as a function of gate bias (same legend), for unpassivated and *in situ* passivated Pd/9 nm(nominal) ALD HfO₂/InGaAs/InP MOS devices. (b) Multiple frequency CV, and inset hysteresis, curves for *in situ* 50 °C H₂S passivated InGaAs MOS device. No capacitance correction was made for inductive and resistive elements in the circuit. The average frequency dispersion of the flatband capacitance C_{fb} , is $<3.5\%$ per decade for all devices. The hysteresis measured around C_{fb} at 100 kHz was 460 mV for the unpassivated device, and 380, 585, and 410 mV for the 50, 200, and 350 °C *in situ* H₂S passivated devices, respectively.

epitaxial layer surface. This has been observed in previous studies of H₂S treatment of GaAs(001).¹⁷ In addition, the fact that H species formed on the surface by H₂S dissociation will be in equilibrium with the H₂ MOVPE carrier gas may assist in allowing H passivation to occur by reducing hydrogen desorption from the surface. The possibility that hydrogen passivation occurs in this process is subject to further investigation.

Figure 3(a) shows a bright field transmission electron microscopy (TEM) micrograph for a 50 °C *in situ* H₂S passivated InGaAs device with a 9.4 nm HfO₂ layer and a 0.8 nm thick interfacial layer (IL) between the HfO₂ and InGaAs. This is less than half the thickness of the IL of 1.9 nm measured by TEM for the unpassivated device [Fig. 3(b)]. This indicates that this *in situ* passivation technique is effective in significantly inhibiting interfacial oxide growth. Considering that the maximum H₂S flow rate was limited to 0.1 SCCM in this MOVPE process, there is scope for refinement and potential improvement of this *in situ* passivation technique.

CV curves for a thickness series of 3, 9.4, and 16.8 nm thick ALD HfO₂ layers on 50 °C *in situ* passivated InGaAs are shown in Fig. 4(a). The inset plots the JV response for the three thicknesses. As expected, the leakage current density at $V_{fb}+1$ V is significantly higher for the 3 nm device, $\sim 2 \times 10^{-6}$ A/cm², compared to $\sim 3 \times 10^{-8}$ A/cm² and 2×10^{-8} A/cm² for the 9.4 and 16.8 nm devices, respectively.

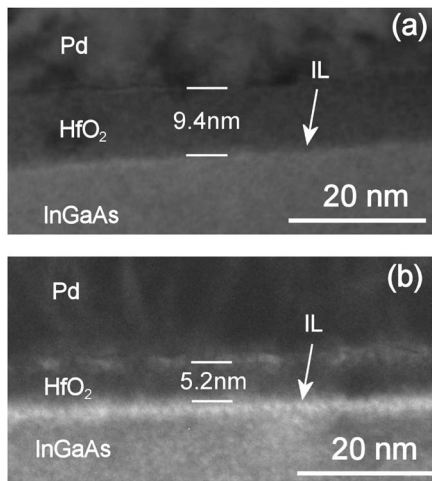


FIG. 3. Bright field TEM micrographs of Pd/9 nm(nominal) ALD HfO_2 /InGaAs/InP MOS devices for (a) *in situ* 50 °C H_2S passivated InGaAs and (b) unpassivated InGaAs. The actual HfO_2 layer [and interfacial layer (IL)] thicknesses measured by TEM were 5.2 nm (1.9 nm IL) unpassivated device, 9.4 nm (0.8 nm IL) 50 °C device, 13.5 nm (0.9 nm IL) 200 °C device, 10.8 nm (0.9 nm IL) 350 °C device, and 11 nm (1.3 nm IL) $(\text{NH}_4)_2\text{S}$ passivated device.

For these HfO_2 layers, we estimate a HfO_2 k value of ~ 23 . Figure 4(b) compares the electrical characteristics of a 9.4 nm thick ALD HfO_2 layer (0.8 nm IL) deposited on InGaAs passivated *in situ* by H_2S flow at 50 °C, and an 11 nm thick ALD HfO_2 layer (1.3 nm IL) on InGaAs passivated *ex situ* in aqueous $(\text{NH}_4)_2\text{S}$. Although a slight V_{fb} shift is apparent, a similar profile is observed in the CV curves of both devices. Both devices have a similar C_{max} in accumulation while the *in situ* passivated device appears to have slightly higher interface state density. The JV plot in the inset of Fig. 4(b) shows similar leakage current density at $V_{fb} + 1$ V with a higher electric breakdown field for the *in situ*

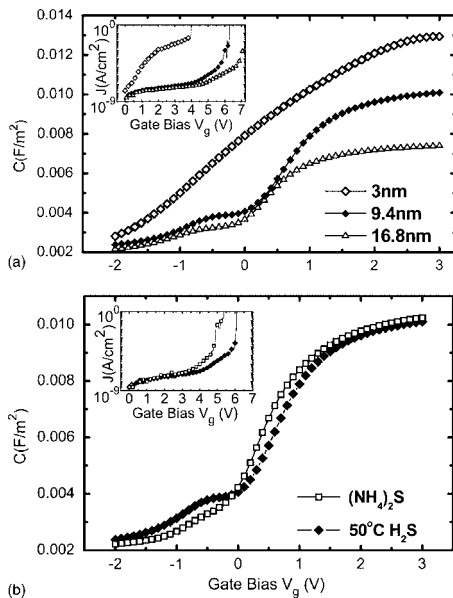


FIG. 4. (a) CV (100 kHz) curves and inset JV (same legend) for nominal 3, 9, and 15 nm thick ALD HfO_2 layers on 50 °C *in situ* passivated InGaAs. The actual HfO_2 (and IL) thicknesses from TEM were 3 nm (0.8 nm IL), 9.4 nm (0.8 nm IL), and 16.8 nm (0.9 nm IL). No significant degradation of the bulk and interface properties is observed after repeated CV measurement of the MOS structures. (b) CV (100 kHz) and inset JV (same legend) characteristics for *in situ* 50 °C H_2S passivated and *ex situ* aqueous $(\text{NH}_4)_2\text{S}$ passivated devices.

passivated device. This demonstrates that the *in situ* passivation approach employed in this work can achieve results comparable to those obtained using *ex situ* aqueous $(\text{NH}_4)_2\text{S}$ passivation.

In summary, we have studied an *in situ* passivation of $\text{In}_{0.53}\text{Ga}_{0.47}\text{As}$ performed using the H_2S dopant source (50–350 °C) at the end of MOVPE growth prior to deposition of ALD HfO_2 . XPS analysis revealed the suppression of As oxide growth on *in situ* passivated InGaAs layers. The MOS device, which experienced a passivation temperature of 50 °C, displays the best electrical characteristics, with TEM indicating a significant reduction in interfacial oxide thickness compared to the unpassivated and $(\text{NH}_4)_2\text{S}$ passivated devices. The potential for developing this passivation approach for use in future CMOS applications is demonstrated by the fact that results comparable to those obtained using *ex situ* aqueous $(\text{NH}_4)_2\text{S}$ passivation can be achieved.

The authors thank Dan O'Connell, Tyndall National Institute, for sample processing. The authors acknowledge useful discussions with Niti Goel, Wilman Tsai, and Marko Radostavljevic, Intel Corporation. The authors would like to acknowledge the following for financial support of this work: Science Foundation Ireland (05/IN/1751); Irish Research Council for Science, Engineering, and Technology, Intel Ireland.

- ¹A. Chen, M. Passlack, N. Medendorp, and D. Braddock, Appl. Phys. Lett. **84**, 2325 (2004).
- ²J. Kwo, M. Hong, B. Busch, D. A. Muller, Y. J. Chabal, A. R. Kortan, J. P. Mannaerts, B. Yang, P. Ye, H. Gossman, A. M. Sergeant, K. K. Ng, J. Bude, W. H. Schulte, E. Garfunkel, and T. Gustafsson, J. Cryst. Growth **251**, 645 (2003).
- ³A. Kortan, M. Hong, J. Kwo, J. P. Mannaerts, and N. Kopylov, Phys. Rev. B **60**, 10913 (1999).
- ⁴T. Ashley, A. R. Barnes, L. Buckle, S. Datta, A. B. Dean, M. T. Emeny, M. Fearn, D. G. Hayes, K. P. Hilton, R. Jefferies, T. Martin, K. J. Nash, T. J. Philips, W. H. A. Tang, P. J. Wilding, and R. Chau, Proceedings of the Seventh International Conference on Solid-State and IC Technology, 2004, pp. 2253–2256.
- ⁵M. Passlack, M. Hong, M. P. Mannaerts, R. L. Opila, S. N. G. Chu, N. Moriya, F. Ren, and J. R. Kwo, IEEE Trans. Electron Devices **44**, 214 (1997).
- ⁶P. D. Ye, G. D. Wilk, J. Kwo, B. Yang, H.-J. L. Gossman, M. Frei, S. N. G. Chu, J. P. Mannaerts, M. Sergeant, M. Hong, K. K. Ng, and J. Bude, IEEE Electron Device Lett. **24**, 209 (2003).
- ⁷Y. Xuan, H. C. Lin, P. D. Ye, and G. D. Wilk, Appl. Phys. Lett. **88**, 263518 (2006).
- ⁸C.-H. Chang, Y.-K. Chiou, Y.-C. Chang, K.-Y. Lee, T.-D. Lin, T.-B. Wu, M. Hong, and J. Kwo, Appl. Phys. Lett. **89**, 242911 (2006).
- ⁹N. Goel, P. Majhi, C. O. Chui, W. Tsai, D. Choi, and J. S. Harris, Appl. Phys. Lett. **89**, 163517 (2006).
- ¹⁰S. Oktyabrsky, V. Tokranov, M. Yakimov, R. Moore, S. Koveshnikov, W. Tsai, F. Zhu, and J. C. Lee, Mater. Sci. Eng., B **135**, 272 (2006).
- ¹¹S. Pal, S. M. Shivaprasad, Y. Aparna, and B. R. Chakraborty, Appl. Surf. Sci. **245**, 196 (2005).
- ¹²K. Kukli, T. Pilvi, M. Ritala, T. Sajavaara, J. Lu, and M. Leskela, Thin Solid Films **491**, 328 (2005).
- ¹³A. Callegari, P. D. Hoh, D. A. Buchanan, and D. Lacey, Appl. Phys. Lett. **54**, 332 (1989).
- ¹⁴N. Goel, P. Majhi, W. Tsai, M. Warusawithana, D. G. Schlom, M. B. Santos, J. S. Harris, and Y. Nishi, Appl. Phys. Lett. **91**, 093509 (2007).
- ¹⁵A. Dimoulas, G. Mavrou, G. Vellianitis, E. K. Evangelou, N. Boukos, M. Houssa, and M. Caymax, Appl. Phys. Lett. **86**, 032908 (2005).
- ¹⁶A. Dimoulas, G. Vellianitis, G. Mavrou, E. K. Evangelou, and A. Sotiropoulos, Appl. Phys. Lett. **86**, 223507 (2005).
- ¹⁷C. H. Chung, S. I. Yi, and W. H. Weinberg, J. Vac. Sci. Technol. A **15**, 1163 (1997).